# CONJUGATE TRANSIENT HEAT TRANSFER IN LAMINAR NATURAL CONVECTION IN A HORIZONTAL CYLINDRICAL ANNULUS

V. I. Bubnovich and P. M. Kolesnikov

UDC 536.25

The conjugate problem of natural convection in a horizontal cylindrical annulus is solved numerically, the solutions are compared with nonconjugate problems, and it is shown that the walls affect the heat transfer in the annular channel.

Natural convection in annular channels formed by concentric cylinders is the subject of intensive research, owing to its widespread application in various engineering apparatuses, e.g., in solar energy converters, plasma accelerators, chemical technological equipment, plasmatrons, etc. [1-3].

It has been observed [4] that flows associated with natural convection in cylindrical annular channels can be divided into four basic types, depending only on the Grashof number and the reciprocal of the relative width of the annular channel. The transition from stable to unstable flow has been investigated over a wide range of reciprocal relative channel widths [5]. Custer and Shaughnessy [6] have studied the solution of the steady-state problem as a function of the Grashof number, the channel width, and the type of temperature boundary conditions at the channel walls for fluids having a very low Prandtl number, using the technique of expanding the numbers $Gr_0$ and Pr in power series. The influence of the Prandtl number on natural-convection heat transfer in horizontal annular channels has been investigated [7]. A numerical study of natural convection in the channels between horizontal eccentric cylinders is reported in [8]. Turbulent natural convection in an annular channel is discussed in [9]. By far the greater majority of the above-cited papers give steady-state solutions of the problem; transient problems are covered in [10-13].

Increasing importance has been attached lately to the solution of conjugate natural-convection problems in closed spaces. Asymptotic methods are used in [14] to solve the steady-state conjugate problem of natural convection in an annular channel between a coaxial hollow cylinder and inner solid cylinder. A detailed bibliography pertaining to numerical, experimental, and theoretical work on natural-convection heat and mass transfer is given in [15].

The objective of the present study is to analyze the influence of the thickness and thermal conductivity of the wall on conjugate natural-convection heat transfer in a horizontal coaxial cylindrical channel.

The geometry of the channel is characterized by the quantities $r_i$, b' and $r_0$, c'. It is assumed that the angle $\varphi$ is measured relative to the vertical downward free-fall acceleration vector and varies within the interval $0° \le \varphi \le 180°$ (Fig. 1). Using a cylindrical coordinate system and neglecting friction heating, we write the dimensionless equations for the problem in the form

$$\frac{\partial \omega}{\partial t} + u\frac{\partial \omega}{\partial R} + \frac{v}{R}\frac{\partial \omega}{\partial \varphi} = \mathrm{Pr}\nabla^2\omega + \mathrm{Gr}_i\mathrm{Pr}^2\left[\sin\varphi\frac{\partial \theta_2}{\partial R} + \frac{\cos\varphi}{R}\frac{\partial \theta_2}{\partial \varphi}\right], \tag{1}$$

$$\omega = -\nabla^2\psi, \tag{2}$$

$$\frac{\partial \theta_2}{\partial t} + u\frac{\partial \theta_2}{\partial R} + \frac{v}{R}\frac{\partial \theta_2}{\partial \varphi} = \nabla^2\theta_2, \tag{3}$$

$$\frac{\partial \theta_1}{\partial t} = \tilde{a}\nabla^2\theta_1, \tag{4}$$

A. V. Lykov Institute of Heat and Mass Transfer, Academy of Sciences of the Belorussian SSR, Minsk. Translated from Inzhenerno-Fizicheskii Zhurnal, Vol. 51, No. 4, pp. 576-583, October, 1986. Original article submitted July 8, 1985.

0022-0841/86/5104-1175$12.50  

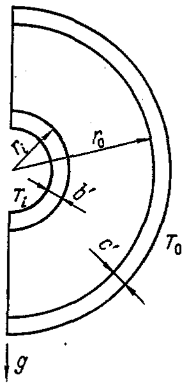


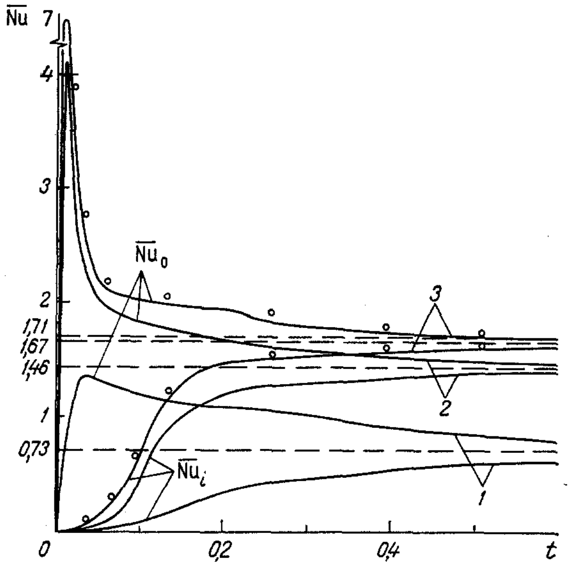


Fig. 1 Fig. 2

Fig. 1. Geometry of the channel.

Fig. 2. Influence of the channel wall thickness on the mean Nusselt numbers in the course of relaxation to the steady state; the points correspond to the solution of the nonconjugate problem ($\overline{Nu}$ = 1.71), $\tilde{\lambda}$ = 0.4, $\tilde{a}$ = 2.0. 1) b = c = 0.4; 2) b = c = 0.1; b = c = 0.01.

where

$$R = r/r_i;\ \omega = \Omega r_i^2/a_2;\ \psi = \Psi/a_2;\ t = a_2\tau/r_i^2;$$
$$\theta = (T - T_0)/(T_i - T_0);\ u = v_r r_i/a_2;\ v = v_\varphi r_i/a_2;$$
$$\tilde{a} = a_1/a_2;\ \mathrm{Pr} = \nu/a_2;\ v = \partial\psi/\partial R;\ u = -R^{-1}\partial\psi/\partial\varphi;\tag{5}$$
$$\mathrm{Gr}_i = g\beta(T_i - T_0)\, r_i^3/\nu^2;\ \nabla^2 = \partial^2/\partial R^2 + R^{-1}\partial/\partial R + R^{-2}\partial^2/\partial\varphi^2.$$

We adopt the initial and boundary conditions

$$u = v = \psi = \omega = \theta_1 = \theta_2 = 0 \text{ at } \quad t = 0,\tag{6}$$

$$\psi = \frac{\partial^2\psi}{\partial\varphi^2} = \omega = \frac{\partial\theta_1}{\partial\varphi} = \frac{\partial\theta_2}{\partial\varphi} = 0 \text{ along } \ \varphi = 0,\ \pi,\tag{7}$$

$$\left.\begin{aligned}&\psi = \partial\psi/\partial R = 0\\ &\theta_1 = \theta_2,\ \frac{\partial\theta_1}{\partial R} = \tilde{\lambda}\,\frac{\partial\theta_2}{\partial R}\end{aligned}\right\} \text{ for } \quad R = 1, \qquad R = \eta,\tag{8}$$

$$\theta_1 = 1 \text{ for } \ R = 1 - b,\quad \theta_1 = 0 \text{ for } \ R = \eta + c.\tag{9}$$

The vorticity boundary condition at the walls is determined from Eq. (2):

$$\omega = -\partial^2\psi/\partial R^2.\tag{10}$$

The system of equations (1)-(4) and boundary conditions (8)-(10) involves parameters that are induced in the problem by the conjugation of the temperature fields at the fluid–wall boundary:

1) the ratio of the thermal conductivities of the fluid and the wall $\tilde{\lambda} = \lambda_2/\lambda_1$;

2) the ratio of the thermal diffusivities of the wall and the fluid $\tilde{a} = a_1/a_2$;

3) relative channel wall th icknesses $b = b'/r_i$ and $c = c'/r_i$.

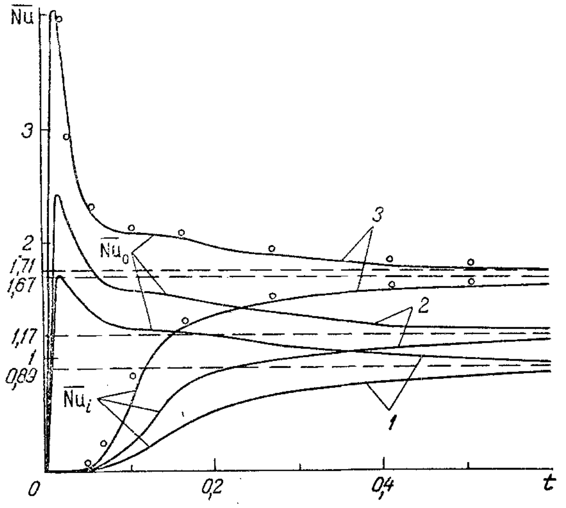


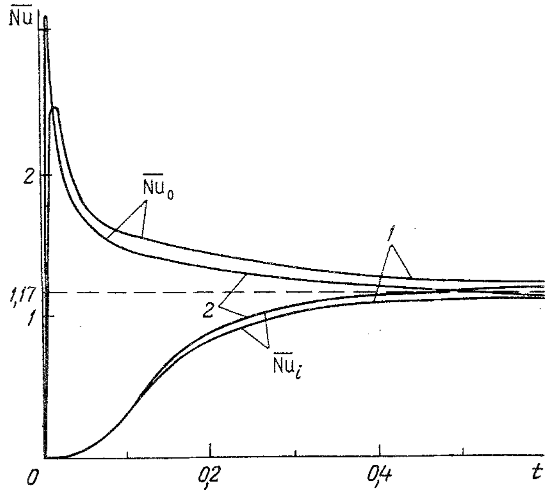


Fig. 3 Fig. 4

Fig. 3. Influence of the ratio of the thermal conductivities of the fluid and channel walls on the mean Nusselt numbers in the transient thermal convection regime; the points correspond to the solution of the nonconjugate problem, b = c = 0.2, $\tilde{a}$ = 2.0. 1) $\tilde{\lambda}$ = 0.8; 2) 0.4; 3) 0.02.

Fig. 4. Influence of the ratio of the thermal diffusivities of the channel walls and the fluid on the mean Nusselt numbers in the transient thermal convection regime, b = c = 0.2, $\tilde{\lambda}$ = 0.4. 1) $\tilde{a}$ = 2; 2) 500.

The parameters $Gr_i$, Pr, $\tilde{\lambda}$, $\tilde{a}$, $\eta$, b, c in our work are varied between the following limits: $200 \le Gr_i \le 38800$; $0.02 \le Pr \le 0.7$; $0.02 \le \tilde{\lambda} \le 0.8$; $2 \le \tilde{a} \le 500$; $1.5 \le \eta \le 5$; $0.01 \le b \le 0.4$; $0.01 \le c \le 0.4$.

The system of equations (1)-(4) with the initial conditions (6) and the boundary conditions (7)-(10) are solved numerically on an implicit finite-difference scheme by the method of alternating directions [16]. A 21 × 19 computing grid is used; it is uniform with respect to the angle $\varphi$ and is variable with respect to the radius R, the points becoming more closely spaced toward the walls. The convection terms in Eqs. (1) and (3) are represented by asymmetric first-order upwind-differencing equations [16].

We write the finite-difference analogs of the differential equations (1)-(4) for interior points:

$$\frac{\omega_{kj}^{n+1/2}-\omega_{kj}^{n}}{\Delta t/2}+(u_{kj}^{n}-|u_{kj}^{n}|)\,\frac{\omega_{kj+1}^{n+1/2}-\omega_{kj}^{n+1/2}}{2\Delta R_j}+(u_{kj}^{n}+|u_{kj}^{n}|)\times$$
$$\times\frac{\omega_{kj}^{n+1/2}-\omega_{kj-1}^{n+1/2}}{2\Delta R_{j-1}}+(v_{kj}^{n}-|v_{kj}^{n}|)\,\frac{\omega_{k+1j}^{n}-\omega_{kj}^{n}}{2R_j\Delta\varphi}+(v_{kj}^{n}+|v_{kj}^{n}|)\times$$
$$\times\frac{\omega_{kj}^{n}-\omega_{k-1j}^{n}}{2R_j\Delta\varphi}=\Pr\left[\left(R_{j+1}\,\frac{\omega_{kj+1}^{n+1/2}-\omega_{kj}^{n+1/2}}{\Delta R_j}-\right.\right.$$
$$\left.\left.-R_j\,\frac{\omega_{kj}^{n+1/2}-\omega_{kj-1}^{n+1/2}}{\Delta R_{j-1}}\right)/(R_j\Delta R_j)+\frac{\omega_{k+1j}^{n}-2\omega_{kj}^{n}+\omega_{k-1j}^{n}}{R_j^2\,\Delta\varphi^2}\right]+$$
$$+\operatorname{Gr}\Pr^2\left[\frac{\theta_{2\ kj+1}^{n}-\theta_{2\ kj-1}^{n}}{R_{j+1}-R_{j-1}}\sin\varphi_k+\frac{\cos\varphi_k}{R_j}\,\frac{\theta_{2\ k+1j}^{n}-\theta_{2\ k-1j}^{n}}{2\Delta\varphi}\right], \tag{11}$$
$$\frac{\omega_{kj}^{n+1}-\omega_{kj}^{n+1/2}}{\Delta t/2}+(u_{kj}^{n}-|u_{kj}^{n}|)\,\frac{\omega_{kj+1}^{n+1/2}-\omega_{kj}^{n+1/2}}{2\Delta R_j}+$$
$$+(u_{kj}^{n}+|u_{kj}^{n}|)\,\frac{\omega_{kj}^{n+1/2}-\omega_{kj-1}^{n+1/2}}{2\Delta R_{j-1}}+(v_{kj}^{n}-|v_{kj}^{n}|)\,\frac{\omega_{k+1j}^{n+1}-\omega_{kj}^{n+1}}{2R_j\Delta\varphi}+$$
$$+(v_{kj}^{n}+|v_{kj}^{n}|)\,\frac{\omega_{kj}^{n+1}-\omega_{k-1j}^{n+1}}{2R_j\Delta\varphi}=\Pr\left[\left(R_{j+1}\,\frac{\omega_{kj+1}^{n+1/2}-\omega_{kj}^{n+1/2}}{\Delta R_j}-\right.\right.$$

$$- R_j \frac{\omega_{kj}^{n+1/2} - \omega_{kj-1}^{n+1/2}}{\Delta R_{j-1}} \Big) / (R_j \Delta R_j) + \frac{\omega_{k+1j}^{n+1} - 2\omega_{kj}^{n+1} + \omega_{k-1j}^{n+1}}{R_j^2 \Delta\varphi^2} \Big] +$$

$$+ \mathrm{Gr}_i \Pr^2 \left[ \frac{\theta_{2\,kj+1}^n - \theta_{2\,kj-1}^n}{R_{j+1} - R_{j-1}} \sin\varphi_k + \frac{\cos\varphi_k}{R_j} \frac{\theta_{2\,k+1j}^n - \theta_{2\,k-1j}^n}{2\Delta\varphi} \right], \tag{12}$$

$$\frac{\overset{s+1/2}{\psi}{}_{kj}^{n+1} - \overset{s}{\psi}{}_{kj}^{n+1}}{\varepsilon/2} - \Big( R_{j+1} \frac{\overset{s+1/2}{\psi}{}_{kj+1}^{n+1} - \overset{s+1/2}{\psi}{}_{kj}^{n+1}}{\Delta R_j} -$$

$$- R_j \frac{\overset{s+1/2}{\psi}{}_{kj}^{n+1} - \overset{s+1/2}{\psi}{}_{kj-1}^{n+1}}{\Delta R_{j-1}} \Big) / (R_j \Delta R_j) - (\overset{s}{\psi}{}_{k+1j}^{n+1} - 2\overset{s}{\psi}{}_{kj}^{n+1} + \overset{s}{\psi}{}_{k-1j}^{n+1}) / (R_j \Delta\varphi)^2 = \omega_{kj}^{n+1}, \tag{13}$$

$$\frac{\overset{s+1}{\psi}{}_{kj}^{n+1} - \overset{s+1/2}{\psi}{}_{kj}^{n+1}}{\varepsilon/2} - \Big( R_{j+1} \frac{\overset{s+1/2}{\psi}{}_{kj+1}^{n+1} - \overset{s+1/2}{\psi}{}_{kj}^{n+1}}{\Delta R_j} -$$

$$- R_j \frac{\overset{s+1/2}{\psi}{}_{kj}^{n+1} - \overset{s+1/2}{\psi}{}_{kj-1}^{n+1}}{\Delta R_{j-1}} \Big) / (R_j \Delta R_j) - (\overset{s+1}{\psi}{}_{k+1j}^{n+1} - 2\overset{s+1}{\psi}{}_{kj}^{n+1} + \overset{s+1}{\psi}{}_{k-1j}^{n+1}) / (R_j \Delta\varphi)^2 = \omega_{kj}^{n+1}, \tag{14}$$

$$\frac{\theta_{2\,kj}^{n+1/2} - \theta_{2\,kj}^n}{\Delta t/2} + (u_{kj}^n - |u_{kj}^n|) \frac{\theta_{2\,kj+1}^{n+1/2} - \theta_{2\,kj}^{n+1/2}}{2\Delta R_j} + (u_{kj}^n + |u_{kj}^n|) \times$$

$$\times \frac{\theta_{2\,kj}^{n+1/2} - \theta_{2\,kj-1}^{n+1/2}}{2\Delta R_{j-1}} + (v_{kj}^n - |v_{kj}^n|) \frac{\theta_{2\,k+1j}^n - \theta_{2\,kj}^n}{2R_j \Delta\varphi} + (v_{kj}^n + |v_{kj}^n|) \times$$

$$\times \frac{\theta_{2\,kj}^n - \theta_{2\,k-1j}^n}{2R_j \Delta\varphi} = \Big( R_{j+1} \frac{\theta_{2\,kj+1}^{n+1/2} - \theta_{2\,kj}^{n+1/2}}{\Delta R_j} - \tag{15}$$

$$- R_j \frac{\theta_{2\,kj}^{n+1/2} - \theta_{2\,kj-1}^{n+1/2}}{\Delta R_{j-1}} \Big) / (R_j \Delta R_j) + \frac{\theta_{2\,k+1j}^n - 2\theta_{2\,kj}^n + \theta_{2\,k-1j}^n}{R_j^2 \Delta\varphi^2},$$

$$\frac{\theta_{2\,kj}^{n+1} - \theta_{2\,kj}^{n+1/2}}{\Delta t/2} + (u_{kj}^n - |u_{kj}^n|) \frac{\theta_{2\,kj+1}^{n+1/2} - \theta_{2\,kj}^{n+1/2}}{2\Delta R_j} +$$

$$+ (u_{kj}^n + |u_{kj}^n|) \frac{\theta_{2\,kj}^{n+1/2} - \theta_{2\,kj-1}^{n+1/2}}{2\Delta R_{j-1}} + (v_{kj}^n - |v_{kj}^n|) \frac{\theta_{2\,k+1j}^{n+1} - \theta_{2\,kj}^{n+1}}{2R_j \Delta\varphi} +$$

$$+ (v_{kj}^n + |v_{kj}^n|) \frac{\theta_{2\,kj}^{n+1} - \theta_{2\,k-1j}^{n+1}}{2R_j \Delta\varphi} = \Big( R_{j+1} \frac{\theta_{2\,kj+1}^{n+1/2} - \theta_{2\,kj}^{n+1/2}}{\Delta R_j} - \tag{16}$$

$$- R_j \frac{\theta_{2\,kj}^{n+1/2} - \theta_{2\,kj-1}^{n+1/2}}{\Delta R_{j-1}} \Big) / (R_j \Delta R_j) + \frac{\theta_{2\,k+1j}^{n+1} - 2\theta_{2\,kj}^{n+1} + \theta_{2\,k-1j}^{n+1}}{R_j^2 \Delta\varphi^2},$$

$$\frac{\theta_{1\,kj}^{n+1/2} - \theta_{1\,kj}^n}{\Delta t/2} = \tilde{a} \Big[ R_{j+1} \frac{\theta_{1\,kj+1}^{n+1/2} - \theta_{1\,kj}^{n+1/2}}{R_j \Delta R_j^2} - \tag{17}$$

$$- \frac{\theta_{1\,kj}^{n+1/2} - \theta_{1\,kj-1}^{n+1/2}}{\Delta R_{j-1} \Delta R_j} + \frac{\theta_{1\,k+1j}^n - 2\theta_{1\,kj}^n + \theta_{1\,k-1j}^n}{R_j^2 \Delta\varphi^2} \Big],$$

$$\frac{\theta_{1\,kj}^{n+1} - \theta_{1\,kj}^{n+1/2}}{\Delta t/2} = \tilde{a} \Big[ R_{j+1} \frac{\theta_{1\,kj+1}^{n+1/2} - \theta_{1\,kj}^{n+1/2}}{R_j \Delta R_j^2} - \tag{18}$$

$$- \frac{\theta_{1\,kj}^{n+1/2} - \theta_{1\,kj-1}^{n+1/2}}{\Delta R_j \Delta R_{j-1}} + \frac{\theta_{1\,k+1j}^{n+1} - 2\theta_{1\,kj}^{n+1} + \theta_{1\,k-1j}^{n+1}}{R_j^2 \Delta\varphi^2} \Big].$$

The first- and second-order partial derivatives occurring in the boundary conditions (7), (8), (10) are expressed in terms of the following relations in the interior approximation [16].

$$\frac{\partial f}{\partial n} = \frac{-3f_0 + 4f_1 - f_2}{2h} + O(h^2), \tag{19}$$

$$\frac{\partial^2 f}{\partial n^2}=\frac{-7f_0+8f_1-f_2}{2h^2}-\frac{3}{h}\left(\frac{\partial f}{\partial n}\right)\Big|_0+O(h^2), \tag{20}$$

where $u = (\varphi, R)$; $f = (u, \psi, \theta_1, \theta_2)$.

The temperature conjugation conditions (8) on the inner and outer cylinders are transformed into the respective difference equations

$$\theta^n_{1\,kj}=\theta^n_{2\,kj},\quad \frac{\theta^n_{1\,kj}-\theta^n_{1\,kj-1}}{\Delta R_{j-1}}=\tilde{\lambda}\,\frac{\theta^n_{2\,kj+1}-\theta^n_{2\,kj}}{\Delta R_j}\quad \text{for}\quad R=1,$$
$$\theta^n_{2\,kj}=\theta^n_{1\,kj},\quad \tilde{\lambda}\,\frac{\theta^n_{2\,kj}-\theta^n_{2\,kj-1}}{\Delta R_{j-1}}=\frac{\theta^n_{1\,kj+1}-\theta^n_{1\,kj}}{\Delta R_j}\quad \text{for}\quad R=\eta. \tag{21}$$

Equations (13) and (14) involve the relaxation parameter $\varepsilon$, which in our work is chosen according to the condition

$$\varepsilon=\min\left\{\begin{matrix}\Delta R_j\\ \Delta\varphi\end{matrix}\right\}/\pi.$$

With the introduction of the parameter $\varepsilon$ the equation for the stream function (2) is transformed from an elliptic to a parabolic equation.

The computational process for the system of equations (11)-(18) in a given time layer is as follows. First, Eqs. (11) and (12) are solved in succession by a double-sweep procedure, using the values of $u_{kj}{}^n$, $v_{kj}{}^n$, $\theta_{2kj}{}^n$, and $\omega_{kj}{}^n$ from the preceding time n; this operation makes it possible to determine the values of the vorticity $\omega_{kj}{}^{n+1}$ at interior points of the annular channel. Then Eqs. (13) and (14) are solved at those same points by an iterative procedure with the application of separate double sweeps in the R and $\varphi$ directions and the boundary conditions (7) and (8) for $\psi$, whereupon the field of the stream functions is determined in the domain occupied by fluid. The iteration process is terminated upon satisfaction of the convergence test

$$\Sigma\left(|\overset{s+1}{\psi}{}^{n+1}_{kj}-\overset{s}{\psi}{}^{n+1}_{kj}|/|\overset{s+1}{\psi}{}^{n+1}_{kj}|\right)<10^{-3}.$$

The number of required iterations diminishes rapidly from 25-30 immediately after the start of the computations to 2-4 for the majority of the other time steps. The velocity fields are computed from the known $\psi_{kj}{}^{n+1}$ as follows:

$$v^{n+1}_{kj}=\frac{\psi^{n+1}_{kj+1}-\psi^{n+1}_{kj-1}}{R_{j+1}-R_{j-1}},\qquad u^{n+1}_{kj}=\frac{-\psi^{n+1}_{k+1j}+\psi^{n+1}_{k-1j}}{2R_j\Delta\varphi}, \tag{22}$$

and the vorticity at the channel walls is computed according to Eq. (20). Then Eqs. (15)-(18) are solved by means of the conjugation conditions (21) according to a double-sweep procedure, and the temperature field is determined both at the walls and in the fluid, and the local Nusselt numbers for the surfaces of the inner and outer cylinders are determined according to the equations

$$\mathrm{Nu}_i=-\ln(\eta)\left[\frac{\partial\theta_2}{\partial R}\right]\Big|_{R=1},\qquad \mathrm{Nu}_0=-\eta\ln(\eta)\left[\frac{\partial\theta_2}{\partial R}\right]\Big|_{R=\eta}, \tag{23}$$

respectively. Finally, the expressions

$$\overline{\mathrm{Nu}}_i=\frac{1}{\pi}\int_0^\pi \mathrm{Nu}_i\,d\varphi,\qquad \overline{\mathrm{Nu}}_0=\frac{1}{\pi}\int_0^\pi \mathrm{Nu}_0\,d\varphi$$

are used to compute the mean values of the Nusselt numbers for each cylinder. The above-indicated integrals are evaluated numerically with the application of Simpson's rule. The global Nusselt number $\overline{\mathrm{Nu}}$ is determined as the arithmetic mean of $\overline{\mathrm{Nu}}_i$ and $\overline{\mathrm{Nu}}_0$. The computation of one time layer is terminated at this juncture, and the computational process is repeated.

The values of the thermophysical parameters $\lambda$, $\rho$, and $C_p$ at the fluid–wall boundaries are assumed to be equal to the arithmetic mean of their values in the two media.

We have tested the reliability of the foregoing numerical algorithm by comparing the solutions obtained by several authors [5, 6, 10] for nonconjugate problems using the values of the parameters

1) $\mathrm{Pr} = 0.7, \quad \eta = 1.57, \quad \mathrm{Ra} = 14\,420$ [5];

2) $\mathrm{Pr} = 0.01, \quad \eta = 5, \quad \mathrm{Gr}_0 = 200$ [6];

3a) $\mathrm{Pr} = 0.7, \quad \eta = 1.5, \quad \mathrm{Gr} = 4850$ [10];

3b) $\mathrm{Pr} = 0.7, \quad \eta = 2, \quad \mathrm{Gr} = (10\,000,\ 26\,600,\ 38\,800)$ [10]

with the analogous solutions obtained in the present study in the conjugate formulation as $\tilde{\lambda} \to 0$. Excellent agreement of the results is observed here for the flow structure and also for the temperature and velocity profiles. Indicating that the given numerical method is reliable and stable.

Our main concern here is to analyze the variation of the heat-transfer characteristics in an annular channel as the ratios of the thermal conductivities and thermal diffusivities of the walls and fluid and the relative channel wall thicknesses are varied. The Prandtl number is taken equal to 0.7 (air) in the ensuing discussion, the Grashof number is equal to $10^4$, and the ratio of the diameters of the outer and inner cylinders is 2.0. The results of computations performed by the above-described method are shown in Figs. 2-4. It is evident from Fig. 2 that in the steady state for b = c = 0.01 the value of $\overline{\mathrm{Nu}}$ for the conjugate problem differs from its counterpart in the nonconjugate case by 0.04 ($\sim$2%), i.e., they practically coincide for both problems. But then for a wall thickness equal to 0.4, the discrepancy of $\overline{\mathrm{Nu}}$ is appreciable, amounting to 0.98 ($\sim$57%). Moreover, the maximum of the function $\overline{\mathrm{Nu}}_0(t)$ decreases considerably and gradually shifts to the right along the t axis as the channel wall thickness is increased from 0.01 to 0.4.

Figure 3 shows the dependence of the solution on another conjugation parameter $\tilde{\lambda}$ for $\tilde{a}$ = 2.0 and b = c = 0.2. The steady-state data lead to the assertion that allowance for the finite thickness of the channel walls and conjugation of the temperature fields at the fluid–wall boundary decreases the number $\overline{\mathrm{Nu}}$ by 1/1.92 in the transition from $\tilde{\lambda} = 0.02$ to $\tilde{\lambda} = 0.8$. For $\tilde{\lambda} = 0.02$ the mean values of the criterion $\overline{\mathrm{Nu}}$ for the conjugate and the nonconjugate problems differ by 2%.

The parameter $\tilde{a}$ affects the heat-transfer process in the channel only as the solution approaches the steady state, as illustrated in Fig. 4. This influence is so slight, even with a 250-fold increase in $\tilde{a}$, that it can in all probability be neglected. For the special case under consideration, where $\mathrm{Gr}_i$ = 10,000, Pr = 0.7, and $\eta$ = 2.0, it is found that the channel walls and the fluid can be strongly coupled in the thermal sense.

Thus, the common assumption in simplified thermal computations, that the heat-transfer coefficient is independent of the thickness and thermophysical properties of the walls, is not always justified, particularly in the case of a low thermal conductivity or large relative thickness of the channel walls, when the problem must be treated only in the conjugate formulation.

## NOTATION

$a_1$, $a_2$, thermal conductivities of the wall and fluid, respectively; $\tilde{a} = a_1/a_2$; $\tau$, time; t, dimensionless time; b', c', wall thicknesses of inner and outer cylinders; b, c, dimensionless wall thicknesses of inner and outer cylinders; g, free-fall acceleration; $\mathrm{Gr}_i$, $\mathrm{Gr}_0$, Grashof numbers calculated with respect to radii of the inner and outer cylinders; Nu, Nusselt number; $\overline{\mathrm{Nu}}$, mean Nusselt number; Pr, Prandtl number; Ra, Rayleigh number; r, $\varphi$, cylindrical coordinates; R, dimensionless radial coordinate; T, temperature; $v_r$, $v_\varphi$, radial and angular components of velocity; u, v, dimensionless radial and angular velocity components; $\beta$, coefficient of thermal expansion of fluid; $\eta$, ratio of radii of outer and inner cylinders; $\theta$, dimensionless temperature; $\lambda_1$, $\lambda_2$, thermal conductivities of wall and fluid; $\lambda = \lambda_2/\lambda_1$; $\rho$, density of fluid; $\varepsilon$, relaxation parameter; $\Omega$, $\Psi$, vorticity and stream function; $\omega$, $\psi$, dimensionless vorticity and stream function; $r_i/(r_0 - r_i)$, reciprocal of the relative annular channel width. Indices: i, inner cylinder; 0, outer cylinder.

## LITERATURE CITED


1. B. S. Petukhov, L. G. Genin, and S. L. Kovalev, Heat Transfer in Nuclear Power Plants [in Russian], Moscow (1974).
2. P. M. Kolesnikov, Electrodynamic Plasma Acceleration [in Russian], Moscow (1971).
3. A. V. Lykov, Heat-Transfer Handbook [in Russian], Moscow (1978).

4. R. E. Powe, C. T. Carley, and E. H. Bishop, Trans. ASME, Ser. C: J. Heat Transfer, 91, No. 3, 310 (1969).
5. R. E. Powe, C. T. Carley, and S. L. Carruth, Trans. ASME, Ser. C: J. Heat Transfer, 93, No. 2, 210 (1971).
6. J. R. Custer and E. J. Shaughnessy, Trans. ASME, Ser. C: J. Heat Transfer, 99, No. 4, 596 (1977).
7. T. H. Kuehn and R. J. Goldstein, Trans. ASME, Ser. C: J. Heat Transfer, 102, No. 4, 768 (1980).
8. C. H. Cho, K. S. Chang, and K. H. Park, Trans. ASME, Ser. C: J. Heat Transfer, 104, No. 4, 624 (1982).
9. B. Farouk and S. I. Güceri, Trans. ASME, Ser. C: J. Heat Transfer, 104, No. 4, 631 (1982).
10. Y. T. Tsui and B. Tremblay, Int. J. Heat Mass Transfer, 27, No. 1, 103-111 (1984).
11. M. C. Charrier-Mojtabi, A. Mojtabi, and J. P. Caltagironi, Trans. ASME, Ser. C: J. Heat Transfer, 101, No. 1, 171 (1979).
12. B. É. Vasilik, B. B. Petrazhitskii, M. A. Rozanov, and L. N. Shchukin, Tr. Mosk. Énerg. Inst., No. 588, 24-30 (1982).
13. B. Tremblay and Y. T. Tsui, IEEE Trans. Power Appar. Syst., TPAS-103, No. 3, 668-672 (1984).
14. Z. Rotem, Int. J. Heat Mass Transfer, 15, 1679-1693 (1972).
15. O. G. Martynenko and Yu. A. Sokovishin, Natural-Convection Heat and Mass Transfer: Bibliographic Index [in Russian], Parts 1 and 2, Minsk (1982, 1983).
16. V. M. Paskonov, V. I. Polezhev, and L. A. Chudov, Numerical Simulation of Heat- and Mass-Transfer Processes [in Russian], Moscow (1984).

# EXPERIMENTAL STUDY OF THE PROCESS OF ESTABLISHMENT OF PHOTOABSORPTION-INDUCED CONVECTION

V. I. Zuev

UDC 536.252

The times required for establishing photoabsorption-induced convection in a cell containing an absorbing liquid by a vertically propagating laser beam are measured. The results obtained are compared with available theoretical estimates.

1. The absorption of powerful laser radiation in an absorbing medium causes photoabsorption-induced convection (PAC) to appear near the region of heating [1, 2]. The low threshold of PAC distinguishes it from other types of free convection. The laser beam is a unique, stationary, continuous, volume, penetrable source of heat. It has the characteristic feature that as a result of the thermal self-action in the absorbing medium the characteristics of the beam itself change.

The thermalization time of the laser radiation, determined by the molecular absorption time of a radiation quantum in the medium (in this case a liquid) and by the collision time of the molecules, is obviously much shorter than the times characteristic for the appearance of PAC. The times for establishing different states of PAC in a liquid were determined in [3, 4] ($Pr \gg 1$): 1) $t_v = D^2/\chi$ for the case of weak ($Pe \ll 1$, $Re \ll 1$) and moderate ($Pe \gg 1$, $Re \ll 1$) convection; 2) $t_v = D/v$ for developed convection ($Pe \gg 1$, $Re \gg 1$).

It was noted that as the intensity of the beam of heating radiation increases the process of establishing convective motion can acquire an oscillatory character.

Experiments on photoabsorption-induced convection, induced by horizontal [3] and vertical [5] beams of laser radiation in a gas, have been performed. In so doing, however, the velocities of the convective flows were not measured, and the establishment of motion was judged from indirect data.

Institute of Physics of the Atmosphere, Academy of Sciences of the USSR, Moscow. Tranlated from Inzhenerno-Fizicheskii Zhurnal, Vol. 51, No. 4, pp. 584-586, October, 1986. Original article submitted July 25, 1985.